

it is reasonable to drop  $K_{23}$  as well. Then, we obtain

$$\Psi_{\text{im}}' = \Phi + (\epsilon_0 - K_1 - V^{(1)} + i\epsilon)^{-1} V^{(1)} \Phi. \quad (6.2)$$

The essential difference between (6.1) and (6.2) is that (6.1) is a reduction of the original three-body problem to a two-body problem, while (6.2) is practically a one-body problem and thus can be solved in exactly the same way as the functions  $\chi_0$  and  $\Psi_0^{(1)}$ . The model described by (6.2) is the scattering of the particle 1 by the two fixed centers 2 and 3, for each value of fixed  $\mathbf{r}_{23}$ . Again, the distortion effect of  $V^{(1)}$  is taken into account

exactly in the impulse-approximation limit, the recoil of 2 and 3 due to the collision with 1 being included with their relative positions held fixed. The corrections to (6.2), possible modifications to satisfy unitarity, and some applications of the model will be discussed elsewhere.

#### ACKNOWLEDGMENTS

The author wishes to thank Professor A. Russek for several helpful discussions and Professor K. Haller for a discussion on the high-energy scattering model.

## Photodisintegration of the Deuteron by Polarized Gamma Rays

G. BARBIELLINI, C. BERNARDINI, F. FELICETTI, AND G. P. MURTAS

*Laboratori Nazionali di Frascati del Comitato Nazionale per l'Energia Nucleare, Frascati, Italy*

(Received 12 September 1966)

An experiment has been performed on the photodisintegration of the deuteron by linearly polarized  $\gamma$  rays in the energy range from 200 to 400 MeV. The polarization is obtained by the crystal technique and is generally of the order of 30 to 40%. Both the neutron and the proton are detected in coincidence in order to reduce the background drastically. The asymmetry parameter at  $90^\circ$  in the center-of-mass system has been determined as a function of the energy  $k$  of the photon; it depends very little on  $k$  and has a value close to  $-0.3$  all over the range.

### 1. INTRODUCTION

DEUTERON photodisintegration has been extensively investigated in recent years. A complete reference index can be found in the report by Toms.<sup>1</sup>

Experiments above the pion threshold have measured the differential cross section and the distribution of the plane of disintegration by the use of linearly polarized  $\gamma$  rays. The present experiment is concerned with this last kind of measurement in the energy region 200–400 MeV (lab system) of the incident  $\gamma$ -ray beam, that is, around the first nucleon resonance. The present status of knowledge about high-energy deuteron photodisintegration is summarized briefly in the following.

#### A. Theory

At the outset, the photodisintegration problem looks quite similar to the usual photoelectric effect in atoms. There, a knowledge of the static (Coulomb) potential between bound charges allows a very accurate computation of the cross section. Corrections arising from the interaction of the incoming  $\gamma$  ray with additional charges brought in by vacuum polarization do not change appreciably the results concerning the photoelectric effect.

In the case of photodisintegration, however, the presence of charged strong-field particles in the two-nucleon

interaction introduces serious doubts about a description of the process based on the use of a nucleon-nucleon potential. In fact the charge in the deuteron is not strongly localized on the proton, but can travel from one nucleon to the other for a substantial fraction of the time in the form of charged-meson exchange currents. On qualitative grounds it is expected that because of the pion mass, the charge can be considered as localized in general on the nucleons when the frequency  $k$  of the incoming  $\gamma$  ray is such that  $k \ll m_\pi$  ( $\hbar=c=1$ ), that is, when  $k$  is well below the  $\pi$ -meson threshold. Moreover, the nucleon itself can undergo transitions to isobaric states such as the first 33 resonance.

Low-energy theoretical results ( $k < 10$  MeV) are in good agreement with the static-potential picture. A very refined calculation of this kind has recently been performed by Partovi<sup>2</sup> using the well-known multipole-series technique. The number of multipoles involved must be quite large in order to give results accurate to  $k \lesssim 100$  MeV (in the frame of the static-potential picture).

Even a careful analysis like Partovi's (or the recent work including relativistic corrections by Le Bellac, Renard, and Tran Thanh Van<sup>3</sup>) cannot reproduce the high-energy data. A peak appears (see Fig. 1)

<sup>2</sup> F. Partovi, *Ann. Phys. (N. Y.)* **27**, 79 (1964).

<sup>1</sup> M. E. Toms, U. S. Naval Research Laboratory Bibliography No. 24, 1965 (unpublished).

<sup>3</sup> M. Le Bellac, F. M. Renard, and J. Tran Thanh Van, *Nuovo Cimento* **33**, 594 (1964).

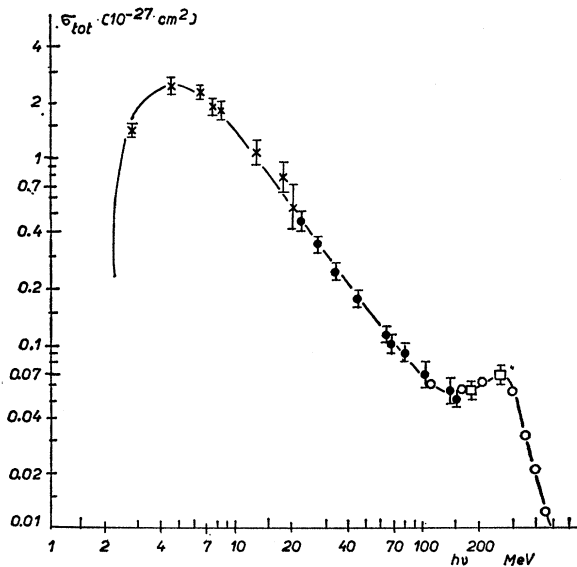


FIG. 1. Total cross section for deuteron photodisintegration as a function of laboratory photon energy.

in the total cross section at  $k=250$  MeV and this seems unambiguously related to the first nucleon resonance  $N^*$ .

After some attempts to interpret the peak on a field-theoretical basis (see Austern<sup>4</sup> and Zachariassen<sup>5</sup>) a phenomenological model by Wilson<sup>6</sup> succeeded in giving a good fit to the total cross section. The phenomenological input to this model is given by the  $\pi$ -photoproduction data together with the assumption that every  $\pi$  is re-absorbed by one of the nucleons if they meet in a given range. This model has the advantage of recognizing the dominance of  $N^*$  and  $S$ -wave production over the classical photoelectric mechanism (the electromagnetic part).

The interpretation of the angular-distribution data appears a bit more complicated. The role of interference terms between the electromagnetic (e.m.) and mesonic contributions is not clear. The same applies to the recent asymmetry data from polarized  $\gamma$  rays (Liu,<sup>7</sup> this experiment).

The asymmetry parameter  $\Sigma(k, \theta)$  is defined by

$$\Sigma(k, \theta) = \frac{d\sigma_{11}(k, \theta) - d\sigma_{\perp}(k, \theta)}{d\sigma_{11}(k, \theta) + d\sigma_{\perp}(k, \theta)}, \quad (1)$$

where  $\theta$  is the c.m. proton angle and  $d\sigma_{11(\perp)}$  is the differential photodisintegration cross section for production plane parallel (orthogonal) to the polarization vector.

The ratio  $d\sigma_{11}/d\sigma_{\perp}$  is obtained from the experimental

yields  $Y_{11,\perp}(P, k, \theta)$  according to the formula

$$\frac{d\sigma_{11}}{d\sigma_{\perp}} = \frac{P(Y_{11} + Y_{\perp}) + Y_{11} - Y_{\perp}}{P(Y_{11} + Y_{\perp}) - Y_{11} + Y_{\perp}},$$

where  $P$  is the polarization of the linearly polarized  $\gamma$  rays.

Concerning this parameter  $\Sigma$ , one can definitely say that the results of calculations including only e.m. contributions markedly disagree with the experimental results at energies  $\gtrsim 80$  MeV.

## B. Experiments

Results on the photodisintegration cross section have been published by many authors. Note in particular in the Toms review<sup>1</sup> the work by Keck and Tollestrup extending to  $k=450$  MeV.<sup>8</sup>

Besides the already mentioned peak at  $k=250$  MeV, the cross section shows a peculiar  $2+3 \sin^2\theta$  behavior as a function of the c.m. proton angle at the resonance. This can be attributed to magnetic dipole absorption, as expected if there is a contribution from the  $N^*$  production.

We are mainly concerned with measurements of the asymmetry parameter  $\Sigma(k, \theta)$  in the energy range in which meson currents play the predominant role. Previous measurements of  $\Sigma$  have been published by Liu<sup>7</sup> for the  $\theta$  values  $45^\circ$ ,  $90^\circ$ ,  $135^\circ$  and for  $k \leq 230$  MeV, that is, just below the resonant peak.

## 2. THE EXPERIMENTAL APPARATUS

A polarized  $\gamma$ -ray beam is one of the facilities of the Frascati electron synchrotron.<sup>9</sup> This beam is obtained by the crystal technique, whereas the beam used by Liu is obtained by the angular-sampling technique.<sup>10</sup> In both cases the head of the  $\gamma$ -ray spectrum is at higher energies than those of the polarized  $\gamma$  rays, so that a selection of the photodisintegration among  $\pi$  photoproduction processes (p.p. $\pi$ ) is desirable when p.p. $\pi$  comes into play. At Frascati the  $\gamma$ -beam pulse length is  $\sim 2$  msec, allowing for neutron-proton coincidences, so that the energy range can be extended to about 400 MeV. At this energy the linear polarization of the  $\gamma$  rays is still fairly good. The counting rate, however, drops sharply as does the cross section (Fig. 1).

The contamination to be expected in the  $p$ - $n$  coincidences due to p.p. $\pi$  has been estimated by using the

<sup>8</sup> Recent data by a group at Bonn [K. H. Kissler, R. Kose, W. Paul, and K. Stockhorst, in *Proceedings of the International Symposium on Electron and Photon Interactions at High Energies*, edited by G. Höhler *et al.* (Deutsche Physikalische Gesellschaft, Hamburg, 1965), Vol. 2, p. 280] disagree with all previous results. As far as we know this discrepancy is not yet understood. Accurate data in the high-energy region ( $500 \leq k \leq 1000$  MeV) have recently been given by R. Ching and C. Schaerf [Phys. Rev. **141**, 1320 (1966)].

<sup>9</sup> G. Barbiellini, G. Bologna, G. Diambri, and G. P. Murtas, Phys. Rev. Letters **9**, 396 (1962).

<sup>10</sup> R. E. Taylor and R. F. Mozley, Phys. Rev. **117**, 835 (1960).

<sup>4</sup> N. Austern, Phys. Rev. **100**, 1522 (1955).

<sup>5</sup> F. Zachariassen, Phys. Rev. **101**, 371 (1956).

<sup>6</sup> R. R. Wilson, Phys. Rev. **104**, 218 (1956).

<sup>7</sup> F. F. Liu, Phys. Letters **11**, 306 (1964); Phys. Rev. **138**, B1443 (1965).

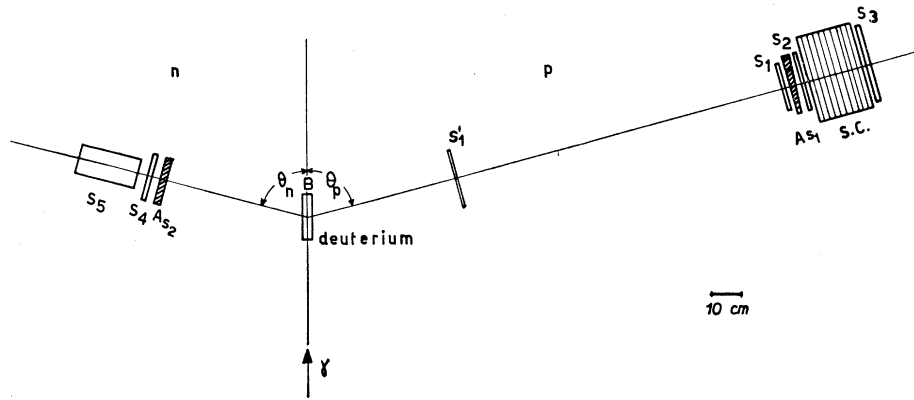


FIG. 2. Experimental apparatus.

total  $p.p.\pi$  cross section<sup>11</sup> and a phase-space distribution of the reaction products. This contamination is completely negligible.

The asymmetry data in this experiment have been taken in two different runs in which both the  $\gamma$ -ray beam and the experimental apparatus were slightly changed. In run No. 1 the polarized beam was obtained by the technique described in Ref. 9. In this run the polarization vector was either parallel or orthogonal to the production plane according to the symbols used in formula (1).

In run No. 2 the crystal orientation was changed to a new working point giving better beam polarization, as suggested by Bologna.<sup>12</sup> In this run, however, the polarization vector was rotated  $13^\circ$  with respect to the

previous axes so that the effective polarization was smaller than expected by a factor  $\cos 26^\circ = 0.90$ .

Figure 2 shows the experimental apparatus used in run No. 2. It consists of a proton range telescope  $S_1'S_1S_2$  (S.C.) ( $S$  are scintillation counters, S.C. is a 31-plate spark chamber) and a neutron counter  $S_4S_5$  on the other side of the target.

In Fig. 3 a block diagram of the electronics is given. The spark chamber was triggered by the master shown in this diagram.

Detailed characteristics of the apparatus are as follows:  $S_1'$  is a 20 by 10 by 0.3  $\text{cm}^3$  plastic scintillator;  $S_1$  is a 16 by 16 by 1  $\text{cm}^3$  plastic scintillator, 160 cm from the target;  $A_{S_1}$  is a wedge-shaped aluminium absorber;  $S_2$  is a 20 by 20 by 0.3  $\text{cm}^3$  plastic scintillator; S.C. is a

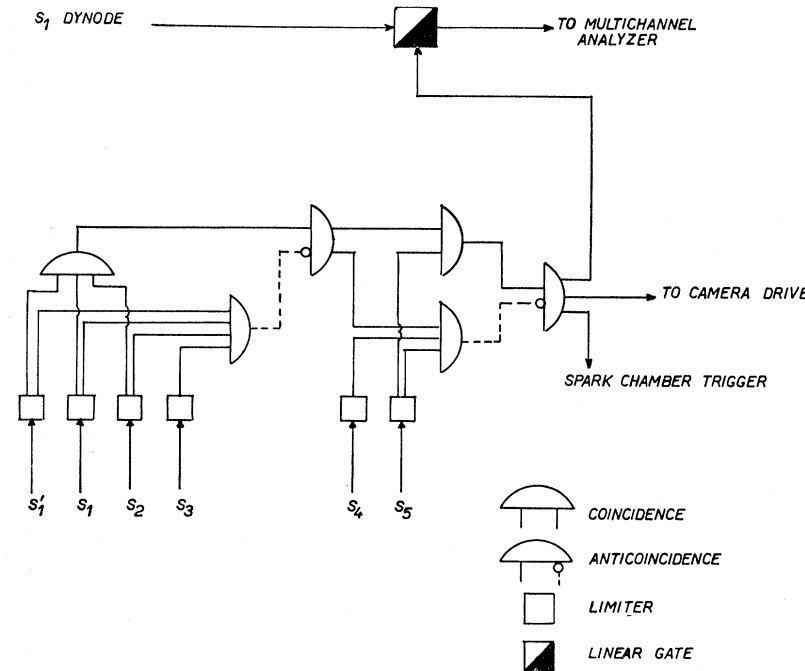


FIG. 3. Block diagram of the electronics.

<sup>11</sup> D. M. White, R. M. Schectman, and B. M. Chasan, Phys. Rev. **120**, 614 (1960).

<sup>12</sup> G. Bologna (private communication).

29 by 29 cm<sup>2</sup> front-area spark chamber, (31 plates, 1-mm Al each);  $\bar{S}_3$  is a 29 by 29 by 1 cm<sup>3</sup> plastic scintillator (in anticoincidence);  $A_{S_2}$  is a 3-cm-thick lead absorber to eliminate soft charged particles;  $\bar{S}_4$  is a 25 by 25 by 1 cm<sup>3</sup> plastic scintillator, 50 cm from the target (in anticoincidence);  $S_5$  is a liquid-scintillator (NE 213) cylindrical neutron counter, 25-cm deep, 20-cm base diam.

In run No. 1 counter  $S_1'$  was not present and counter  $S_2$  was 1.25-cm thick. The addition of  $S_1'$  in run No. 2 gave a better confidence in the performance of the proton telescope by allowing time-of-flight discrimination of the background pions at the lower energies. Discrimination was also checked by pulse-height analysis from  $S_1$ . Both these modifications from run No. 1 to run No. 2 were not strictly necessary. Some overlapping points have been taken in the two runs and they agree well within the statistical errors.

The solid angles and the neutron-counter efficiency have not been accurately determined because ratios of cross sections are not affected by them. (The proton telescope is about 10 msr wide and the neutron-counter efficiency is 10 to 15%. This helps in estimating the counting rate.)

The target was a liquid-deuterium cylinder 15-cm long, with 3-cm base diam.

Because of the near proportionality of the  $\gamma$ -ray energy to the proton kinetic energy, the crystal bremsstrahlung peak can be reproduced in the spark chamber S.C. as a peak in a curve displaying counts versus range. This allows a good energy calibration by comparison of the proton spectrum shape to the one obtained by a pair spectrometer, as shown in Fig. 4.

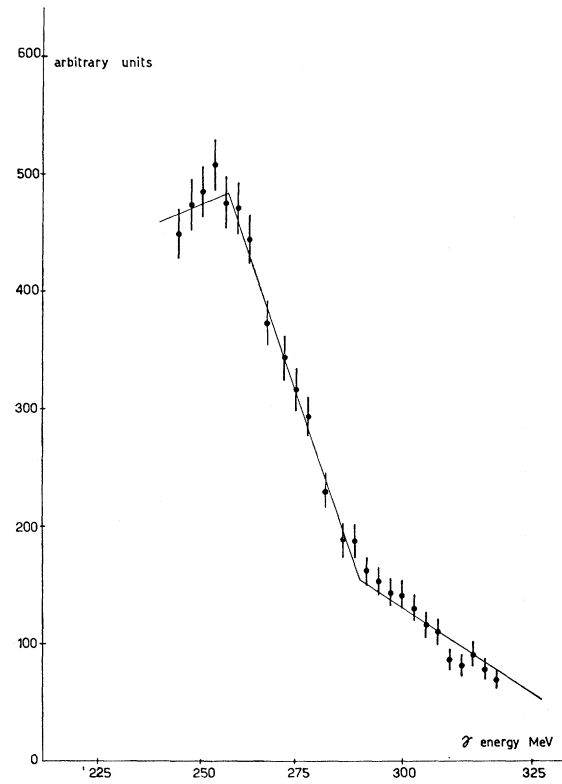


FIG. 4. Typical coherent bremsstrahlung peak as seen by the proton range spectrum in the spark chamber.

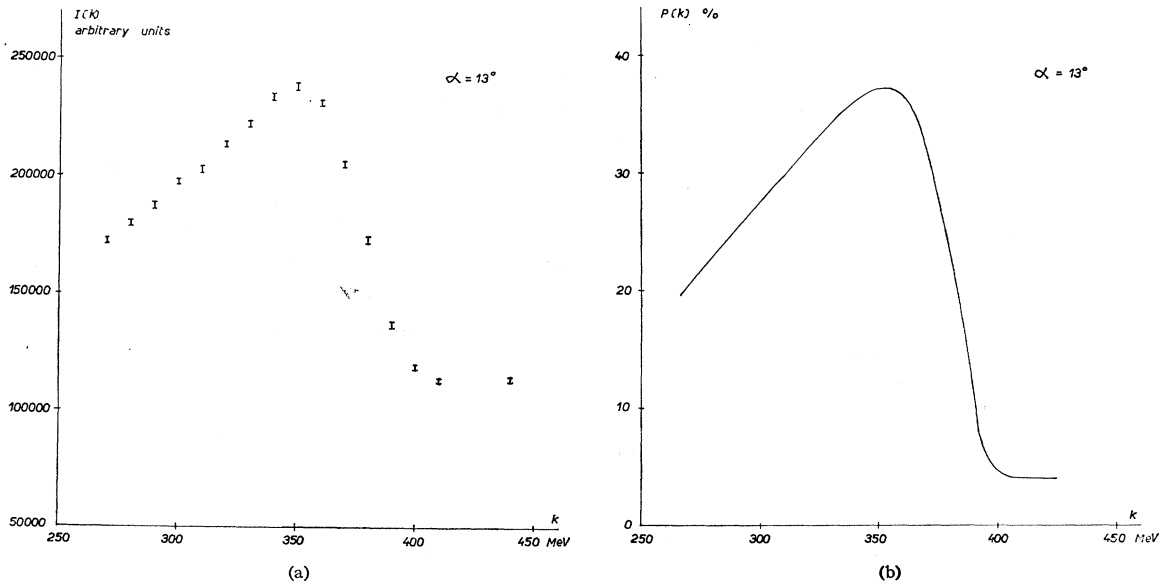


FIG. 5. (a) Typical bremsstrahlung intensity spectrum used in run No. 2 as seen by the pair spectrometer.  $I(k)$  is proportional to the number of photons per unit energy,  $N(k)$ , times the energy  $k$ . (b) Beam polarization as a function of the photon energy corresponding to the spectrum shown in Fig. 5(a).

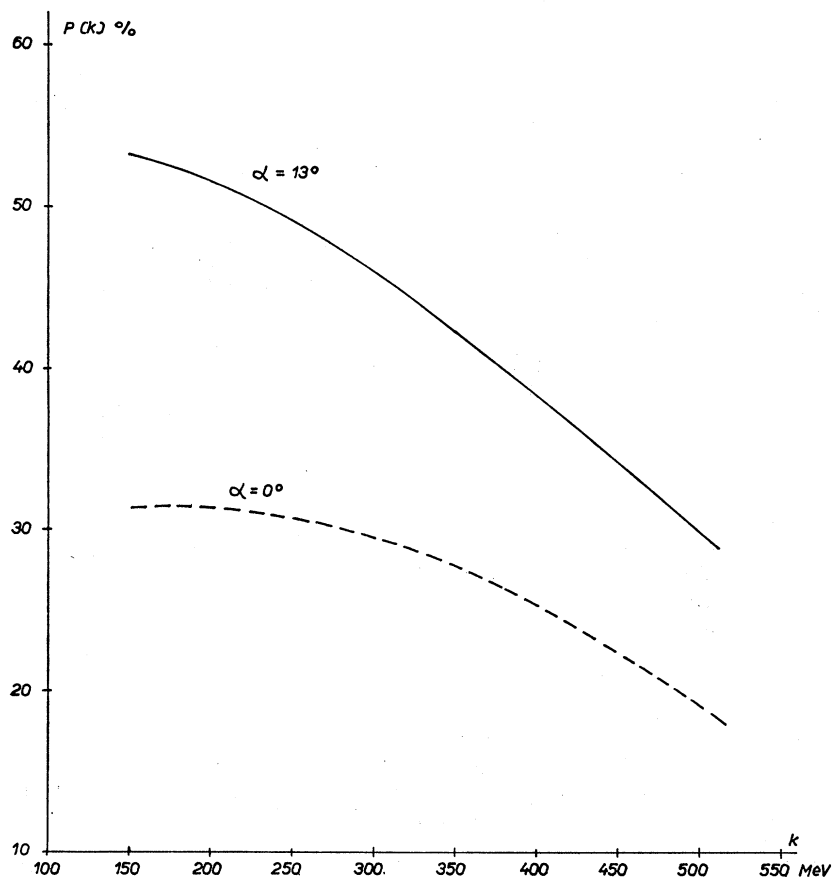


FIG. 6. The peak polarization as a function of the peak photon energy.

### 3. THE POLARIZED $\gamma$ -RAY BEAM

The spectrum and the polarization of the  $\gamma$  rays from the diamond radiator in the synchrotron have been chosen by calculating the orientation of the crystal so that the photons in the coherent peak corresponded to the accepted angle and energy intervals of the proton. The coherent peak was subsequently checked by determining the spectrum with a pair spectrometer. The same spectrum was also checked in one case by reproducing the peak in the spark chamber as shown in Fig. 4.

TABLE I. Experimental results for the asymmetry function  $\Sigma$  at  $\theta=90^\circ$  (c.m. proton angle) for various laboratory photon energies  $k$ , with the error for  $\Sigma$  and  $k$ .  $P$  gives the polarization of the linearly polarized  $\gamma$  rays.

$k$ (MeV)	$P$	$\Sigma$	$\delta\Sigma$	$\Delta k$ (MeV)
235	0.29	0.276	$\pm 0.038$	24
253	0.25	0.330	$\pm 0.090$	19
260	0.37	0.228	$\pm 0.028$	21
277	0.30	0.260	$\pm 0.070$	22
310	0.30	0.350	$\pm 0.040$	11
330	0.34	0.275	$\pm 0.045$	19
380	0.22	0.370	$\pm 0.090$	22
404	0.27	0.340	$\pm 0.110$	24

The polarization was computed following the procedure described in Ref. 9 with the improvements of a more correct atomic model and several experimental corrections (such as multiple scattering and so on), as calculated by Bologna.<sup>12</sup>

Figure 5(a) shows a typical spectrum as used in run No. 2. The polarization corresponding to this spectrum is shown in Fig. 5(b). The behavior of the peak polarization as a function of the peak energy of the coherent bremsstrahlung is also shown in Fig. 6. These curves are labeled  $\alpha=13^\circ$  to indicate the orientation of the polarization vector in run No. 2, as mentioned in Sec. 2.

The peak polarization referring to the crystal parameters in run No. 1 is also shown in Fig. 6, where it is labeled  $\alpha=0^\circ$ .

### 4. RESULTS

By using the experimental apparatus described above, points have been measured giving the asymmetry function  $\Sigma(\theta, k)$  at  $\theta=90^\circ$  (c.m. proton angle) and various laboratory photon energies  $k$ . The data are summarized in Table I. Error estimates on  $P$  have not been included.

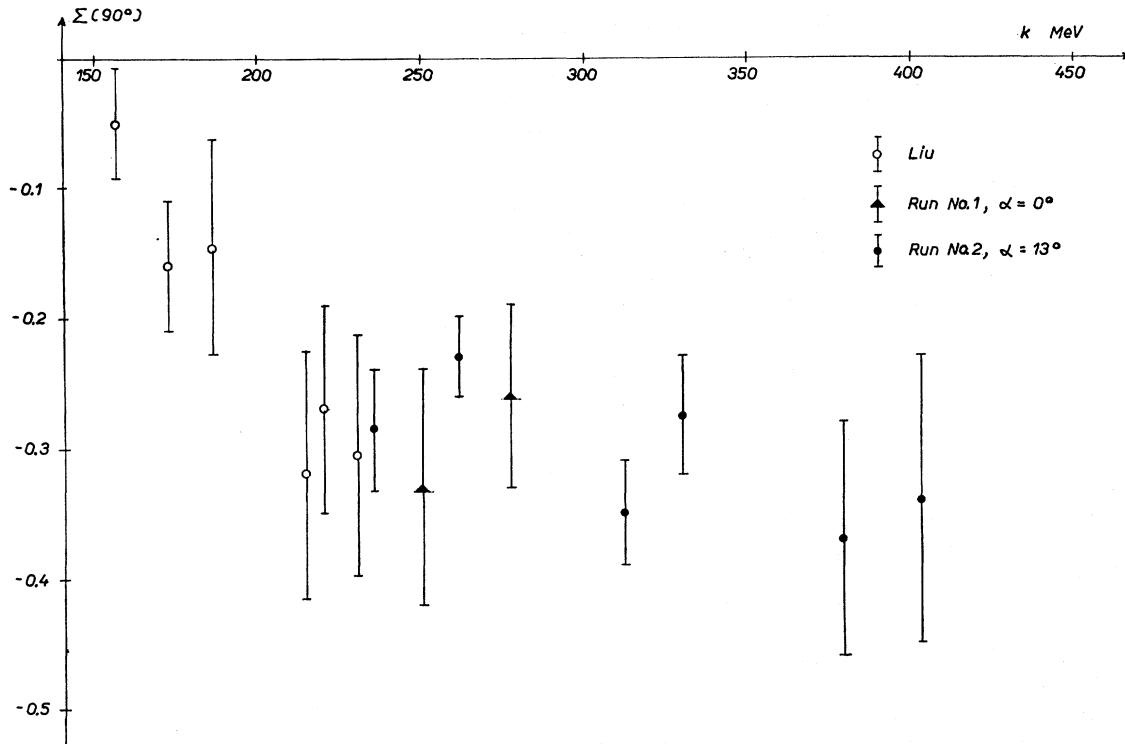


FIG. 7. Experimental results for the asymmetry function  $\Sigma$  at  $90^\circ$  in the c.m. system. Symbols are as follows: hollow circle—Liu (Ref. 7); solid triangle—present experiment, run No. 1; solid circle—present experiment, run No. 2.

The statistical error on  $\Sigma$  has been computed by

$$\frac{\delta\Sigma}{\Sigma} = \frac{[1 - (P\Sigma)^2]^{1/2}}{P\Sigma\sqrt{n}}, \quad (2)$$

where  $n$  is the total number of counts.

The values of the asymmetry parameter  $\Sigma$  in the table have been obtained by averaging over an interval  $\Delta k$  of the energy of the primary  $\gamma$  ray. The value of  $\Delta k$  is given in the table.

The results are also shown in Fig. 7 together with some of the points measured by Liu<sup>7</sup> in the high-energy region.

There is no theoretical prediction for the asymmetry parameter above the first resonance. If the process were dominated by  $\pi$  photoproduction and reabsorption, as suggested by Wilson, the asymmetry in the photodisintegration would bear some resemblance to the corresponding asymmetries in the photoproduction of  $\pi^0$

and  $\pi^+$  (actually a suitable mixture of the two). The presently known results for the photoproduction of  $\pi$ 's are given in Refs. 13–15. We note, finally, that both in the photodisintegration and the photoproduction processes the asymmetry behaves in a similar way, being monotonic and having the same sign over the investigated energy interval.

#### ACKNOWLEDGMENTS

We want to thank G. Bologna for invaluable help in the appropriate choice of the crystal working point and for the reconstruction of the polarization data. We also want to thank B. Bartoli for his collaboration during the first part of this work.

<sup>13</sup> G. Barbiellini *et al.*, in *Proceedings of the 12th Annual International Conference on High-Energy Physics, Dubna, 1964* (Atomizdat, Moscow, 1966), p. 838.

<sup>14</sup> A. Donnachie and G. Shaw, *Ann. Phys. (N. Y.)* **37**, 333 (1966).

<sup>15</sup> P. Gorenstein *et al.*, *Phys. Letters* **19**, 157 (1965); *Phys. Letters* **23**, 394 (1966).